Published in final edited form as:
Biochim Biophys Acta. 2013 January ; 1830(1): 2118–2128. doi:10.1016/j.bbagen.2012.09.020.

Implication of intestinal VDR deficiency in inflammatory bowel disease

Jung-Hwan Kim[1], **Satoshi Yamaori**[1], **Tomotaka Tanabe**[1], **Caroline H. Johnson**[1], **Kristopher W. Krausz**[1], **Shigeaki Kato**[2], and **Frank J. Gonzalez**[1,*]

[1]Laboratory of Metabolism, Center for Cancer Research, National Cancer Institute, National Institutes of Health, Bethesda, Maryland, USA

[2]Institute of Molecular and Cellular Biosciences, University of Tokyo, Tokyo, Japan

Abstract

BACKGROUND—To investigate the function of the intestinal *Vdr* gene in inflammatory bowel disease (IBD), in conjunction with the discovery of possible metabolic markers for IBD using intestine-specific *Vdr* knockout mice.

METHODS— $Vdr^{\Delta IEpC}$ mice were generated, phenotyped and treated with a time-course of 3% dextran sulfate sodium (DSS) to induce colitis. Colitis was diagnosed by evaluating clinical symptoms and intestinal histopathology. Gene expression analysis was carried out. In addition, metabolic markers of IBD were explored by metabolomics.

RESULTS— $Vdr^{\Delta IEpC}$ mice showed abnormal body size, colon structures and feces color. Calcium, collagen, and intestinal proliferation-related gene expression were all decreased, and serum alkaline phosphatase was highly increased. In the acute model which was treated with 3% DSS for six days, $Vdr^{\Delta IEpC}$ mice showed a high score of IBD symptoms; enlarged mucosal layer and damaged muscularis layer. In the recovery experiment model, where mice were treated with 3% DSS for four days and water for three days, $Vdr^{\Delta IEpC}$ mice showed a high score of IBD symptoms; severe damage of mucosal layer and increased expression of genes encoding proinflammatory cytokines. Feces metabolomics revealed decreased concentrations of taurine, taurocholic acid, taurodeoxycholic acid and cholic acid in $Vdr^{\Delta IEpC}$ mice.

CONCLUSIONS—Disruption of the intestinal *Vdr* gene showed phenotypical changes that may exacerbate IBD. These results suggest that VDR may play an important role in IBD.

GENERAL SIGNIFICANCE—VDR function has been implicated in IBD. This is of value for understanding the etiology of IBD and for development of diagnostic biomarkers for IBD.

Keywords

Vitamin D receptor (VDR); inflammatory bowel disease (IBD); bile acids

INTRODUCTION

Inflammatory bowel disease (IBD) is a chronic disorder of the gastrointestinal tract and includes ulcerative colitis and Crohn's disease. Over 1.4 million people in the United States

*Correspondence: Frank J. Gonzalez, gonzalef@mail.nih.gov; Phone: 301-496-9067; Fax: 301-496-8419.

suffer from IBD [1]. Although the etiology of IBD is not fully understood, it is thought to involve a multi-factor interplay of inheritable components, environmental stress, microbial insults and autoimmune events [2–5]. The vitamin D receptor (Vdr), a nuclear hormone receptor, plays an essential role in normal calcium and bone homeostasis. It forms a heterodimer with the retinoid X receptor (Rxr) receptor and binds to the vitamin D response element (VDRE). This is usually found upstream of target genes in the presence of 1,25-dihydroxyvitamin D3 [6]. Recently, genome wide association studies (GWAS) revealed that Vdr could play an important role in over 47 common diseases and traits including Crohn's disease, colorectal cancer and immune-related diseases [7]. Previously, reports have shown important links between Vdr and IBD using the mouse dextran sulfate sodium (DSS)-induced colitis model with whole body *Vdr* knockout mice [8–10]. These reports suggested that Vdr could play a critical role in innate immune responses to IBD. Furthermore, epidemiology studies revealed that calcium and vitamin D supplements could reduce the risk of IBD [11–12]. Thus, Vdr may play an important role in IBD. Although Vdr functions have been implicated in IBD using whole body VDR knockout mice, tissue-specific Vdr functions in IBD have not been investigated. Since Vdr expression may result in different pathophysiology or metabolism in IBD, an intestine-specific *Vdr*-null mouse was generated here to study IBD. In order to evaluate the susceptibility of these mice to colon disease, a DSS-induced colitis model was thus applied [13].

Metabolic perturbations to the intestine-specific *Vdr* knockout mice were analyzed using mass spectrometry-based metabolomics. Metabolomics is rapid, high-throughput, systems biology-based technique that can idenitify all the low molecular-weight metabolites in biofluids, cells, tissues and organisms. Metabolic profiles provide a meaningful snapshot for understanding the metabolic changes that occur following genetic variation, pathophysioloical changes and xenobiotic challenges [14–15], and can show subtle changes between experimental groups. Previously, metabolomics has been applied for the diagnosis of disease [16–17] and the characterization of disease-related animal models [18–20].

METHODS

Materials

DSS (35–44 kDa) was purchased from MP Biomedicals (Aurora, Ohio, USA). Taurine, taurocholic acid, taurodeoxycholic acid, cholic acid, deoxycholic acid and other chemicals were obtained from Sigma-Aldrich (St. Louis, MO, USA). Anti-VDR, anti-COX-2 and anti-actin were purchased from Santa Cruz Biotechnology (Santa Cruz, California, USA). Anti-p-ERK1/2, anti-ERK1/2, anti-p-p65, anti-p65, anti-p-Akt, anti-Akt and secondary antibody were obtained from Cell Signaling Technology (Beverly, MA, USA).

Generation of intestine-specific *Vdr*-null mice

Intestinal epithelial cell-specific *Vdr*-null mice, designated $Vdr^{\Delta IEpC}$, were generated by crossing *Vdr*-floxed mice, designated $Vdr^{F/F}$, with mice carrying the villin-Cre transgene [21]. Villin-Cre transgenic mice were provided by Deborah L. Gumucio (University of Michigan). Cre-mediated recombination resulted in the deletion of exon 2 of the *Vdr* gene. The male mice ($Vdr^{flox/WT}$; Villin-Cre+) F1 mice were interbred with female $Vdr^{flox/flox}$ littermates lacking Villin-Cre. All mice were genotyped by polymerase chain reaction (PCR). $Vdr^{flox/flox}$; Villin-Cre (designated $Vdr^{\Delta IEpC}$) and $Vdr^{flox/flox}$; Villin-Cre^{-} ($Vdr^{F/F}$) mice were used for the following experiments. PCR genotyping for the *Vdr* floxed and recombined alleles were carried out using specific designed primers, *Vdr* Lm, 5′-TCT GAC TCC CAC AAG TGT ACC ACG G-3′ and *Vdr* WTL2, 5′-ATG GAC AGG AAC ACA CAG CAT CA-3′. PCR amplicon sizes for the floxed and non-floxed wild-type were 337 bp and 254 bp, respectively. Mouse tails were genotyped using the following designed primers,

Vdr TEI fVDR S2, 5′-CAA CCT TGG TGA GCT GAG TTT AC-3′, VDR TEI f *Vdr* AS2, 5′-CAC AGC AGG AGT GGG ATT ACT GAT ATT-3′, and *Vdr* in3 flox AS, 5′-TGA CAG TGC CCT GTT CTT CC-3′. PCR amplicon sizes for the wild-type mice, floxed mice and knockout mice were 491 bp, 575 bp and 323 bp, respectively. Amplification of the microsomal epoxide hydrolase gene as a control was carried out as described previously [22]. Conditional knockout of the *Vdr* gene in the different organs was verified by Southern blotting. All experiments were performed with 6- to 10-week-old male and female C57BL/6 background $Vdr^{F/F}$ and Vdr^{IEpC} mice. To assure genetic homogeneity between the $Vdr^{F/F}$ and $Vdr^{\Delta IEpC}$ mice they were interbred for more than ten generations and littermates used in all experiments. Mice were housed in a pathogen-free animal facility under standard 12 hour light/dark cycle with water and chow *ad libitum*. All experiments were carried out under the Association for Assessment and Accreditation of Laboratory Animal Care guidelines with approval from the NCI Animal Care and Use Committee.

Southern blotting

To verify the status of the conditional knockout of the *Vdr* gene from different organs, genomic DNA (1 μg/lane) isolated from small intestine, colon, cecum, stomach, brain and kidney was digested with EcoRI and subjected to Southern blotting as described previously [23]. A random ^{32}P-labeled *Vdr* DNA probe was used for the targeting for 4.3 kb of floxed and 1.8 kb of null.

Serum chemistry

Serum samples were analyzed for calcium, phosphate, ALT, bone specific ALP (bALP), ALP, Cholesterol (CHL) and total bilirubin (TBIL) using a VetScan® comprehensive diagnostic profile kit (ABAXIS, Union City, CA, USA)

DSS-induced colitis

Ten-week-old mice were used to assess the symptoms of DSS-induced colitis under conditions of significant phenotypic changes such as body weight. This was to allow the maximal range of changes in various end-points of colitis after DSS. It was not possible to choose mice for the study that had the same body weight for the two groups as the mouse ages would be very different. The only age in which the mice have a similar body weight would be at 3–4 weeks which is too young for DSS treatment. Thus, pathophysiologically quantifiable symptoms that arise from the phenotypical changes in the $Vdr^{\Delta IEpC}$ mice can be observed by comparing mice of the same age. Mice were administered 3% (w/v) DSS in drinking water for a number of time-points. Daily changes in body weight and pathological signs of colitis, including rectal bleeding and diarrhea, were assessed and recorded as the disease activity index (DAI) on a scale from 0 to 4. Colon samples were collected immediately following CO_2 asphyxiation.

Quantitative real-time PCR

Total RNA were isolated from fresh colon using Trizol (Invitrogen, Carlsbad, CA). Complementary DNA (cDNA) was synthesized from 1 μg total RNA using a SuperScript II reverse transcriptase kit (Invitrogen, Carlsbad, CA). qPCR was performed using an Applied Biosystems Prism 7900HT Sequence Detection System (Foster City, CA). All reactions were performed in a 10 μl volume consisting of 25 ng cDNA, 300 nM of each primer and 5 μl of SYBER Green PCR Master Mix (Applied Biosystems) at 95 °C for 10 min and 40 cycles of 95 °C for 3 s and 60 °C for 30 s. Expression levels of mRNA were normalized to β-actin as the internal standard. Primers for the qPCR were designed using qPrimerDepot (http://mouseprimerdepot.nci.nih.gov).

Microarray analysis

Colon cDNAs were hybridized to Agilent 44K mouse 60-mer oligo microarrays (Agilent Technologies; Santa Clara, CA). Microarray data were processed and analyzed using Genespring GX 10.0 software (Agilent Technologies). Genes that were changed ≥ 2.0-fold with p-values ≤ 0.05 were analyzed through the use of Ingenuity Pathways Analysis (Ingenuity® Systems, www.ingenuity.com).

Western blotting

Scraped colon mucosal layers (proximal to distal) were lysed with RIPA lysis buffer (150mM NaCl, 0.5% Triton X-100, 50mM Tris–HCl, pH 7.4, 25mM NaF, 20mM EGTA, 1mM DTT, 1mM Na_3VO_4 and protease inhibitor cocktail) for 30 min on ice, followed by centrifugation at 14,800 g for 15 min. Protein concentration was measured with bicinchoninic acid (BCA) reagent. Protein (30 μg) was electrophoresed on a 4–15% gradient tris-HCl gel (Bio-Rad, Hercules, CA) and electrotransferred onto a polyvinylidene difluoride membrane in tris-glycine buffer (pH 8.4) containing 20% methanol. The membrane was blocked with 5% fat-free dry milk in phosphate buffered saline containing 0.1% Tween-20 (PBST) for 1 h. The membranes were probed with primary antibodies and horseradish peroxidase-conjugated secondary antibodies using standard western blotting procedures. Proteins were visualized using the femto signal chemiluminescent substrate (Pierce) under the image analyzer (Alpha Innotech Corp., San Leandro, CA).

Histological and immunohistochemical analysis

For microscopic and macroscopic examination of colon damage, colons were opened longitudinally, flushed with PBS, and fixed in 10% buffered formalin. After colon length measurement, colons were prepared using a ‘Swiss roll’ method [24] and embedded in paraffin. The tissue sections (4 μm) were stained with hematoxylin and eosin (H&E) or/and Alcian Blue (Sigma-Aldrich, St. Louis, MO, USA). A monoclonal anti-PCNA antibody was used as a marker for cell proliferation (Santa Cruz Biotechnology, Santa Cruz, California, USA).

LC-MS Analysis of Mouse feces

Ten-week-old male mice were placed in metabolic cages for 24 h and feces collected. The feces (100 mg) samples were freeze-dried, mixed with 1 ml MeOH and centrifuged at 18,000g for 20 min at 4°C. The supernatant was diluted five times with MeOH containing 5 μM chloropropamide as an internal standard and transferred to UPLC vials. A pooled sample containing 5 μl of each sample was also used for quality control. An aliquot (5 μl) was injected onto an ultra performance liquid chromatography electrospray ionization quadrupole time-of-flight mass spectrometry (UPLC-ESI-QTOFMS) system (Waters). An Acquity UPLC BEH C18 column (Waters) was used to separate feces metabolites. The mobile phase flow rate was 0.5 ml/min, with a gradient mobile phase of 0.1% formic acid (A) and methanol (B), also containing 0.1% formic acid. A flow rate of 0.5 ml/min was maintained thru a 10 min run using the following gradient: initial 98% A held for 1.5 min to 40% A at 12 min to 1% A at 18 min, held for an additional minute before equilibrating to initial conditions. Mass spectrometry was performed on a Waters®QTof-Premier™-MS operating in negative electrospray ionization (ESI) mode.

Data processing and multivariate data analysis

Centroided and integrated chromatographic mass data from 50 to 850 m/z were processed by MarkerLynx® (Waters) to generate a multivariate data matrix. Pareto-scaled MarkerLynx matrices including information on sample identity were analyzed by partial least squares discriminate analysis (PLS-DA) using SIMCA-P+ 12 (Umetrics, Kinnelon, NJ). The

loadings scatter S-plots and the contribution lists were used to describe the candidate markers that were significantly different between $VDR^{F/F}$ and $Vdr^{\Delta IEpC}$ mice. Further confirmation of identity was then carried out by repeating the tandem MS fragmentation using authentic standards at 100 μM in MeOH and in feces.

Statistical analysis

Experimental values are expressed as mean ± SD. Statistical analysis was performed by two-tailed Student's t test for unpaired data, with $p < 0.05$ considered statistically significant.

RESULTS

Generation of intestinal specific *VDR* conditional knockout mice and its phenotypes

To investigate the function of Vdr in intestinal diseases, *Vdr*-floxed mice were subjected to *Vdr* exon 2 recombination by use of the villin-Cre transgene. This was to produce an intestine-specific *Vdr* knockout mouse line (Suppl. Fig. 1A). To confirm tissue-specific knockout of the *Vdr* gene, different tissues were genotyped revealing that only the intestinal *Vdr* gene was disrupted. Additionally, the villin-Cre transgene completely disrupted the *Vdr* gene expression in the colon compared to other sections of the intestine (Suppl. Fig. 1B). Conventional southern blotting was also carried out by digesting genomic DNA from different tissues using E*coRI* (Suppl. Fig 1C). Different target sizes of the DNA fragments (4.3kb for floxed and 1.8 kb for null) were probed (Suppl. Fig. 1D).

Phenotypes of intestinal-specific *VDR* conditional knockout mice

The average body weight and size of the male $Vdr^{\Delta IEpC}$ mice was smaller than that of the $Vdr^{F/F}$ mice at 11-weeks of age (Fig. 1A). The body weight of the $Vdr^{\Delta IEpC}$ mice gradually decreased when they reached 5-weeks of age. At 12-weeks of age, there was a large difference in body weight between the $Vdr^{F/F}$ and $Vdr^{\Delta IEpC}$ mice (Fig. 1B). The mice were killed at 12-weeks of age as advised in the animal protocol. This was to prevent excessive distress that could have arisen from the observed body weight decrease and hypoactivity. To determine the effect of intestinal *Vdr* disruption on colon epithelial cell morphology, H&E and Alcian blue staining were carried out on colon tissues from the $Vdr^{F/F}$ and $Vdr^{\Delta IEpC}$ mice. No significant change was seen between the basic structures of the colons from the two mouse models. However, the thickness of the colon mucosal layer in the $Vdr^{\Delta IEpC}$ mice was significantly reduced (Fig. 1C and D) and the colon length was longer than in the control mice (Fig. 1E). To determine whether intestinal VDR could affect the bone calcium metabolism, bone structure of distal femur was examined by H&E staining revealing abnormal cartilage and trabecular structures in the $Vdr^{\Delta IEpC}$ mice (Fig. 1F).

Analysis of serum chemistry

To determine the effect of intestinal *Vdr* disruption on possible organ damage, serum chemistry was performed on $Vdr^{F/F}$ and $Vdr^{\Delta IEpC}$ mice. In the $Vdr^{\Delta IEpC}$ mice, calcium and phosphate concentrations were significantly decreased and ALP levels significantly increased, in particular as mice became older. ALT, bALP, CHL and TBIL levels showed no significant changes in 11-week-old mice, thus suggesting that intestinal *Vdr* disruption resulted in malabsorption of calcium and phosphate from the intestine. Increased ALP levels with no changes to bALP levels could affect liver physiology, potentially resulting in bile duct injury (Fig. 2).

Analysis of calcium, collagen, intestinal proliferation and toll-like receptor-related gene expression levels in $Vdr^{F/F}$ and $Vdr^{\Delta IEpC}$ mice

Based on the DNA microarray data derived from colon of $Vdr^{F/F}$ and $Vdr^{\Delta IEpC}$ mice, mRNAs encoded by genes involved in calcium mobilization, collagen synthesis, intestinal cell proliferation and toll-like receptors (TLRs) were measured. Expression *of Vdr, TrpV6 and S100g* mRNA (calcium-related) were significantly decreased in $Vdr^{\Delta IEpC}$ mice (Fig. 3A). Expression of *Fn, Co1a1* and *Col4a2* mRNA (collagen-related) were also decreased in the $Vdr^{\Delta IEpC}$ mice (Fig. 3B), but only *Col4a2* was significantly decreased. *Retnlb* mRNA (intestinal proliferation related) was also decreased in $Vdr^{\Delta IEpC}$ mice (Fig. 3C). However, there were no significant changes in *Tlr4* and *Traf6* mRNAs (TLR related) in the $Vdr^{\Delta IEpC}$ mice (Fig. 3D). Thus, the lack of Vdr in the intestinal epithelium resulted in an abnormal colon size and mucosal layer. Other gene changes are shown in Figure 4.

Discovery of possible colon disease markers associated with VDR deficiency

As an approach to discover novel metabolic markers for Vdr expression in intestine-specific *Vdr* deficient mice, feces samples were collected from $Vdr^{F/F}$ and $Vdr^{\Delta IEpC}$ mice. The feces color was markedly different between the $Vdr^{F/F}$ and $Vdr^{\Delta IEpC}$ mice, dark brown and pale yellowish grey, respectively (Fig. 5A). The feces was prepared and analyzed by UPLC-ESI-QTOFMS and multivariate data analysis. Partial least squares-discriminant analysis (PLS-DA) was carried out and feces samples collected from the $Vdr^{F/F}$ and $Vdr^{\Delta IEpC}$ mice showed distinct fecal metabolomes (Fig. 5A). Orthogonal projection to latent structures-discriminant analysis (OPLS-DA) models were subsequently made and a number of metabolites correlated to each mouse model were seen (Fig. 5B). The OPLS-DA s-plot shows the correlation (y axis) and covariance (x axis) of each ion to with respect to each class i.e $Vdr^{F/F}$ y=0 and $Vdr^{\Delta IEpC}$ y=1. It also removes any variation not related to the class therefore leaving only discriminatory metabolites important for class determination. The ions that were highly correlated to each mouse model (class) were subjected to tandem MS. They were positively identified as cholic acid, taurine, taurocholic acid and taurodeoxycholic acid after comparison to authentic standards (data not shown), and were increased in the $Vdr^{F/F}$ mice.

Decreased concentrations of taurine and taurine conjugated bile acids in the $Vdr^{\Delta IEpC}$ mice indicated a disruption of taurine metabolism. Therefore mRNA encoding the taurine transporter, Slc6a6, and mRNAs encoded by two other taurine metabolism related genes, *Gad1* and *Ggt1,* were quantified from colon tissue. *Slc6a6* and *Gad1* mRNA level showed no significant difference between the two lines, while *Ggt1* mRNA level was significantly decreased in $Vdr^{\Delta IEpC}$ mice (Fig. 5C). These results suggested that VDR may play an important role in taurine metabolic pathway by regulating the expression of *Ggt1.* The taurine metabolic pathways were generated using the KEGG (Kyoto Encyclopedia of Genes and Genomes) system (Suppl. fig 2).

The relative abundance of deoxycholic acid and cholic acid were measured by targeted quantitation from extracted ion chromatograms. The ratio between was calculated as a high DCA/CA ratio was previously proposed to be a marker for colon disease [25]. The DCA/CA ratio was significantly higher in the $Vdr^{\Delta IEpC}$ mice (Fig. 5D), suggesting that $Vdr^{\Delta IEpC}$ mice could be susceptible to colon disease.

Susceptibility of intestinal $Vdr^{\Delta IEpC}$ mice to experimental DSS-induced IBD

$Vdr^{\Delta IEpC}$ mice showed an increased susceptibility to 3% DSS-induced IBD compared to $Vdr^{F/F}$ mice. At day six after treatment with 3% DSS, the body weight of $Vdr^{\Delta IEpC}$ mice was significantly reduced compared to $Vdr^{F/F}$ mice. The percent of body weight loss between $Vdr^{F/F}$ and $Vdr^{\Delta IEpC}$ mice was 9.5 ± 5.3% and 17.9 ± 5.2%, respectively (Fig. 6A).

Vdr$^{\Delta IEpC}$ mice also showed higher diarrhea and rectal bleeding scores than *Vdr*$^{F/F}$ mice (Fig. 6B and C). Histological analysis of the distal colon in the *Vdr*$^{\Delta IEpC}$ mice revealed an enlarged mucosal layer and goblet cells were expended (Fig. 6D). Severe damage to the muscularis layer was seen (Fig. 6E, inset) and was quantified (Fig. 6E). H&E staining revealed that this layer was eroded by 3% DSS (Fig. 6F).

Expression of mRNAs encoding cytokines and other proinflammatory markers were also analyzed. While *Ifn-γ, Ccr2, Il-10, Il-1β,* and *Cox-2* mRNA levels were not different between the two groups of mice, *Tnf-α, Mcp-1* and *Il-6* mRNAs were significantly increased in each littermate of the *Vdr*$^{\Delta IEpC}$ mice at day six after 3% DSS treatment (Fig. 6G). Western blot results showed no significant difference in COX-2, pERK1/2, pp65 protein levels between the two groups at day six after 3% DSS treatment (Suppl. Fig 3A).

Recovery after challenge of DSS on *Vdr*$^{\Delta IEpC}$ mice

To assess the recovery of IBD after DSS challenge, *Vdr*$^{F/F}$ and *Vdr*$^{\Delta IEpC}$ mice were treated with 3% DSS for four days and replaced with regular water until day seven. The percent of body weight loss was not significantly different between the *Vdr*$^{F/F}$ and *Vdr*$^{\Delta IEpC}$ mice at day seven (Fig. 7A). However, the *Vdr*$^{\Delta IEpC}$ mice showed a significantly higher diarrhea score than the *Vdr*$^{F/F}$ mice at days five and six in this experimental model (Fig. 7B). Rectal bleeding was also severe in the *Vdr*$^{\Delta IEpC}$ mice at days five and six while at day seven, rectal bleeding was not evident in both groups (Fig. 7C).

Vdr$^{\Delta IEpC}$ mice had severe damage to the middle part of their mucosal layer when analyzed by histology, compared to *Vdr*$^{F/F}$ mice. Immunohistochemistry with anti-Pcna, a proliferation marker, showed a random distribution of damage in the mucosal layer of the *Vdr*$^{\Delta IEpC}$ mouse intestine (Fig. 7D). This suggests that the recovery rate of the mucosal layer might be affected by VDR.

Gene expression of proinflammatory cytokines were measured in the recovery model experiments. *Il-6, Ifn-γ, Ccr2* and *Mcp-1* mRNAs were all induced by DSS treatment but there were no significant differences in mRNA levels between the *Vdr*$^{\Delta IEpC}$ and *Vdr*$^{F/F}$ mice. However, *Tnf-α* and *Il-1β* mRNAs were both significantly increased in *Vdr*$^{\Delta IEpC}$ compared to *Vdr*$^{F/F}$ mice (Fig. 7E). These results suggested that Tnf-α and Il-1β may be involved in TLR4 signaling. Hence, mRNAs related to TLR signaling such as those encoded by the *Elk1*, *Tlr4* and *Traf6* genes in *Vdr*$^{\Delta IEpC}$ and *Vdr*$^{F/F}$ mice were measured. *Tlr4* and *Traf6* mRNAs were significantly increased in *Vdr*$^{\Delta IEpC}$ mice (Fig. 7F), suggesting that bacterial lipopolysaccharides (LPS) could aggravate DSS-induced IBD in *Vdr*$^{\Delta IEpC}$ mice. Western blot analysis further showed that the basal level of pAkt was increased and stimulated by DSS treatment in *Vdr*$^{\Delta IEpC}$ mice. Cox-2 and pp65 proteins were significantly induced by DSS treatment in the two groups but no difference was seen between them (Suppl. Fig 3B).

DISCUSSION

The role of intestinal *Vdr* in IBD was investigated through the generation of a novel *Vdr*$^{\Delta IEpC}$ mouse model [26–27]. Intestinal-specific disruption of *Vdr* in the *Vdr*$^{\Delta IEpC}$ mouse line could aid in understanding tissue-specific pathophysiology related to *Vdr* expression and the function of *Vdr* in IBD. The main phenotypic change observed between the *Vdr*$^{\Delta IEpC}$ and *Vdr*$^{F/F}$ mice, was a lower body weight in the *Vdr*$^{\Delta IEpC}$ mice; the same phenotypic change was also seen when comparing whole body *Vdr*-null to *Vdr*$^{F/F}$ mice. The lower body weight could be explained by calcium absorption that occurs in the intestine. Since Vdr functions in whole body calcium homeostasis, disruption of the *Vdr* gene could elicit this phenotypic change. A previous study which dosed calcium in the form of a dietary

supplement to rats revealed that increased calcium intake ameliorated the symptoms of IBD by improving intestinal resistance, and also strengthening the mucosa barrier [11]. A calcium-enriched diet may be able to restore the phenotype. In Figure 1B, body weight between the wild-type and $Vdr^{\Delta IEpC}$ mice mice showed no significant changes. The body weight changes occurred only after weaning of the mice. Thus calcium in the mother's milk might delay the hypocalcemia in the $Vdr^{\Delta IEpC}$ mice mice. Therefore, intestinal calcium absorption could affect the physiology of the intestinal mucosal barrier. Large changes to the mucosal layer thickness were observed in the $Vdr^{\Delta IEpC}$ mouse model and its structure was changed after DSS treatment, resulting in severe ulcerative colitis. The colitis seen may have arisen due to a number of factors, such as increased sensitivity in the innate immune system or destabilization of connective tissues in the colon.

The innate immune system may be a critical factor for IBD. Under normal conditions, a highly developed immune system can protect against intestinal infection, however, disruption of the innate immune system by intestinal microbes can cause severe intestinal diseases, such as ulcerative colitis and Crohn's disease [28]. TLR host receptors on epithelial cells, monocytes, macrophages and dendritic cells [29–30] are part of the innate immune system, and can recognize pathogenic compounds such as LPS, peptideogycanes, flagellin and lipoprotein [31–32]. As shown in this study, TLR-mediated cytokines Tnfα and Il-6, were highly expressed in the DSS-induced colitis model and their expression levels were augmented in $Vdr^{\Delta IEpC}$ mice. In addition another anti-inflammatory cytokine Il-10 has previously been implicated in IBD where Vdr/Il-10 double knockout mice showed severe IBD and mortality [8], however Il-10 was not different here between the mice.

Goblet cells in IBD can also show changes and have been implicated in ulcerative colitis and Crohn's disease [33–34]. The colon goblet cells in the $Vdr^{\Delta IEpC}$ mice were highly saturated in the small mucosal columnar. Goblet cells function to produce mucin which helps the clearance of bacteria and prevents bacterial colonization, and as such have been implicated in gastrointestinal protection. Mucin also serves as a neutralizing agent in the acidic environment of the luminal colon. The high saturation of goblet cells seen in the $Vdr^{\Delta IEpC}$ mice may be due to hypersensitivity from continuous bacterial stress which could have resulted from weakened connective tissue or impaired tight junctions between the cells, followed by abnormal expansion of goblet cells and abnormal structure of mucosal columnar shape after DSS treatment. In addition, microarray revealed that $Vdr^{\Delta IEpC}$ mice had down-regulation of genes relating to the connective tissue/muscular system (data not shown). Thus, collagen-related gene expression could be critical in IBD. Impairment of the muscularis layer may have been the result of down-regulated collagen related-genes, such as *Fn, Co1a1* and *Col4a2*.

Metabolomics analysis was used as a tool to reveal low molecular weight markers for IBD. In this study, depletion of fecal taurine and taurine-conjugated bile acids, taurocholic acid and taurodeoxycholic acid were seen in the $Vdr^{\Delta IEpC}$ mice. Taurine is a sulfur-containing amino acid and has numerous biological roles including bile acid conjugation, antioxidation, immunomodulation, osmoregulation and regulation of calcium levels, which are all affected here in the $Vdr^{\Delta IEpC}$ mice [35]. In mammals, taurine is synthesized in the pancreas via the cystein sulfinic pathway and found in colon. Here, we measured mRNAs encoding enzymes involved in taurine metabolism in colon samples based on the microarray results and KEGG pathway analysis (http://www.genome.jp/kegg/). As shown in a previous report [36], taurine can ameliorate the symptoms of IBD. In addition, taurine play an important role in anti-inflammation by protecting the issues against the toxic effect of myeloperoxidase (MPO)-derived HOCl/OCl^- [37]. Also taurine showed protective effect on TNBS-induced IBD in rat model [38] by reducing the MPO activity and superoxide production. Furthermore, taurine can scavenge the reactive HOCl to form taurochloramine [39–40]. Therefore, taurin

has been implicated on the modulation of IBD by scavenging HOCL. Thus, as shown in the present metabolomics, lack of taurine production may be susceptible to DSS-induced IBD in $Vdr^{\Delta IEpC}$ mice. Furthermore, Gad1 and Ggt1 mRNA expression may support the reduced taurine metabolism in the $Vdr^{\Delta IEpC}$ mice. Thus taurine metabolism may be important in colon in the pathogenesis of IBD.

Depletion of taurine in the $Vdr^{\Delta IEpC}$ mice could be the result of a concomitant decrease in bile acid concentration; since taurine is required for bile acid conjugation, its production could be decreased through a feedback regulatory mechanism. This is also supported by the observation of decreased expression of taurine synthesis related genes. Conversely, Vdr may affect the expression of taurine synthesis genes and thus would in turn affect the conjugation of bile acids. However, an increase in unconjugated bile acids was not observed. There may also be some interplay between calcium-related genes that were downregulated in the $Vdr^{\Delta IEpC}$ mice. Indeed, previous studies have shown that disruption of the taurine transporter gene (*Slc6a6*, also called *Taut*) resulted in decreased healing in blood-borne infections and increased TNF-α, IL-1β and NF-κB after malaria infection in *Taut*-null mice [41]. However there was no difference observed in the expression of *Slc6a6* between the $Vdr^{F/F}$ and $Vdr^{\Delta IEpC}$ mice, but an increase in *Tnfα* was noted. In addition, experiments in the rat have shown that taurine can ameliorate the symptoms of IBD [36]. Thus, the depletion of taurine after *Vdr* disruption may affect the severity of IBD in $Vdr^{\Delta IEpC}$ mice. Furthermore, reports have shown that activation of the intestinal bile acid nuclear receptor, farnesoid X receptor, repressed inflammatory cytokines Tnfα and Il-1β and prevented epithelial permeability and loss of goblet cells in the DSS-colitis model [42–43]. Also, bile acid ratios have also been suggested to be applicable for evaluating intestinal diseases [25]. Taken together, taurine and bile acid appear to have important roles in IBD and require further investigation.

This study has utilized a metabolomics approach to identify perturbed metabolites in an induced model of colitis in the $Vdr^{\Delta IEpC}$ mouse model. These metabolites indicated upstream gene expression level changes and could also be useful as biomarkers for IBD. Disruption of the intestinal *Vdr* gene resulted in changes to body size, blood chemistry, colon structure, bile acid excretion and cytokine gene expression. Hence, the critical functions of the intestinal *Vdr* gene on IBD were revealed.

CONCLUSIONS

Disruption of the intestinal *Vdr* gene in mice resulted in changes to body size, blood chemistry, colon structure, bile acid excretion and cytokine gene expression. These factors combined could exacerbate IBD. Taken together, the results suggest that Vdr may play an important role in IBD.

Supplementary Material

Refer to Web version on PubMed Central for supplementary material.

Acknowledgments

Supported by the National Cancer Institute Intramural Research Program.

ABBREVIATION

VDR	vitamin D receptor

IBD	inflammatory bowel disease
ALP	alkaline phosphatase
ALT	alanine aminotransferase
qPCR	quantitative polymerase chain reaction
UPLC-ESI-QTOFMS	ultra-performance liquid chromatography-electrospray ionization-quadrupole time-of-flight mass spectrometry
DSS	dextran sulfate sodium
CHL	cholesterol
TBIL	total bilirubin
PCNA	proliferating cell nuclear antigen
LPS	lipopolysaccharides
FXR	farnesoid X receptor
H&E	hematoxylin and eosin

References

1. Podolsky DK. Inflammatory bowel disease. N Engl J Med. 2002; 347:417–429. [PubMed: 12167685]
2. Loftus EV Jr. Clinical epidemiology of inflammatory bowel disease: Incidence, prevalence, and environmental influences. Gastroenterology. 2004; 126:1504–1517. [PubMed: 15168363]
3. Schreiber S, Hampe J. Genomics and inflammatory bowel disease. Curr Opin Gastroenterol. 2000; 16:297–305. [PubMed: 17031092]
4. Levine AD, Fiocchi C. Immunology of inflammatory bowel disease. Curr Opin Gastroenterol. 2000; 16:306–309. [PubMed: 17031093]
5. Xavier RJ, Podolsky DK. Unravelling the pathogenesis of inflammatory bowel disease. Nature. 2007; 448:427–434. [PubMed: 17653185]
6. Bouillon R, Carmeliet G, Verlinden L, van Etten E, Verstuyf A, Luderer HF, Lieben L, Mathieu C, Demay M. Vitamin D and human health: lessons from vitamin D receptor null mice. Endocr Rev. 2008; 29:726–776. [PubMed: 18694980]
7. Ramagopalan SV, Heger A, Berlanga AJ, Maugeri NJ, Lincoln MR, Burrell A, Handunnetthi L, Handel AE, Disanto G, Orton SM, Watson CT, Morahan JM, Giovannoni G, Ponting CP, Ebers GC, Knight JC. A ChIP-seq defined genome-wide map of vitamin D receptor binding: associations with disease and evolution. Genome Res. 2010; 20:1352–1360. [PubMed: 20736230]
8. Froicu M, Weaver V, Wynn TA, McDowell MA, Welsh JE, Cantorna MT. A crucial role for the vitamin D receptor in experimental inflammatory bowel diseases. Mol Endocrinol. 2003; 17:2386–2392. [PubMed: 14500760]
9. Kong J, Zhang Z, Musch MW, Ning G, Sun J, Hart J, Bissonnette M, Li YC. Novel role of the vitamin D receptor in maintaining the integrity of the intestinal mucosal barrier. Am J Physiol Gastrointest Liver Physiol. 2008; 294:G208–216. [PubMed: 17962355]
10. Froicu M, Cantorna MT. Vitamin D and the vitamin D receptor are critical for control of the innate immune response to colonic injury. BMC Immunol. 2007; 8:5. [PubMed: 17397543]
11. Schepens MA, Schonewille AJ, Vink C, van Schothorst EM, Kramer E, Hendriks T, Brummer RJ, Keijer J, van der Meer R, Bovee-Oudenhoven IM. Supplemental calcium attenuates the colitis-related increase in diarrhea, intestinal permeability, and extracellular matrix breakdown in HLA-B27 transgenic rats. J Nutr. 2009; 139:1525–1533. [PubMed: 19535420]
12. Kumari M, Khazai NB, Ziegler TR, Nanes MS, Abrams SA, Tangpricha V. Vitamin D-mediated calcium absorption in patients with clinically stable Crohn's disease: a pilot study. Mol Nutr Food Res. 2010; 54:1085–1091. [PubMed: 20306476]

13. Okayasu I, Hatakeyama S, Yamada M, Ohkusa T, Inagaki Y, Nakaya R. A novel method in the induction of reliable experimental acute and chronic ulcerative colitis in mice. Gastroenterology. 1990; 98:694–702. [PubMed: 1688816]

14. Nicholson JK, Lindon JC, Holmes E. 'Metabonomics': understanding the metabolic responses of living systems to pathophysiological stimuli via multivariate statistical analysis of biological NMR spectroscopic data. Xenobiotica. 1999; 29:1181–1189. [PubMed: 10598751]

15. Griffin JL. The Cinderella story of metabolic profiling: does metabolomics get to go to the functional genomics ball? Philos Trans R Soc Lond B Biol Sci. 2006; 361:147–161. [PubMed: 16553314]

16. Brindle JT, Antti H, Holmes E, Tranter G, Nicholson JK, Bethell HW, Clarke S, Schofield PM, McKilligin E, Mosedale DE, Grainger DJ. Rapid and noninvasive diagnosis of the presence and severity of coronary heart disease using 1H-NMR-based metabonomics. Nat Med. 2002; 8:1439–1444. [PubMed: 12447357]

17. Sato Y, Suzuki I, Nakamura T, Bernier F, Aoshima K, Oda Y. Identification of a new plasma biomarker of Alzheimer's disease using metabolomics technology. J Lipid Res. 2012; 53:567–576. [PubMed: 22203775]

18. Chen C, Shah YM, Morimura K, Krausz KW, Miyazaki M, Richardson TA, Morgan ET, Ntambi JM, Idle JR, Gonzalez FJ. Metabolomics reveals that hepatic stearoyl-CoA desaturase 1 downregulation exacerbates inflammation and acute colitis. Cell Metab. 2008; 7:135–147. [PubMed: 18249173]

19. Dumas ME, Barton RH, Toye A, Cloarec O, Blancher C, Rothwell A, Fearnside J, Tatoud R, Blanc V, Lindon JC, Mitchell SC, Holmes E, McCarthy MI, Scott J, Gauguier D, Nicholson JK. Metabolic profiling reveals a contribution of gut microbiota to fatty liver phenotype in insulin-resistant mice. Proc Natl Acad Sci U S A. 2006; 103:12511–12516. [PubMed: 16895997]

20. Jones GL, Sang E, Goddard C, Mortishire-Smith RJ, Sweatman BC, Haselden JN, Davies K, Grace AA, Clarke K, Griffin JL. A functional analysis of mouse models of cardiac disease through metabolic profiling. J Biol Chem. 2005; 280:7530–7539. [PubMed: 15546876]

21. Madison BB, Dunbar L, Qiao XT, Braunstein K, Braunstein E, Gumucio DL. Cis elements of the villin gene control expression in restricted domains of the vertical (crypt) and horizontal (duodenum, cecum) axes of the intestine. J Biol Chem. 2002; 277:33275–33283. [PubMed: 12065599]

22. Hayhurst GP, Lee YH, Lambert G, Ward JM, Gonzalez FJ. Hepatocyte nuclear factor 4alpha (nuclear receptor 2A1) is essential for maintenance of hepatic gene expression and lipid homeostasis. Mol Cell Biol. 2001; 21:1393–1403. [PubMed: 11158324]

23. Granvil CP, Yu AM, Elizondo G, Akiyama TE, Cheung C, Feigenbaum L, Krausz KW, Gonzalez FJ. Expression of the human CYP3A4 gene in the small intestine of transgenic mice: in vitro metabolism and pharmacokinetics of midazolam. Drug Metab Dispos. 2003; 31:548–558. [PubMed: 12695342]

24. Moolenbeek C, Ruitenberg EJ. The "Swiss roll": a simple technique for histological studies of the rodent intestine. Lab Anim. 1981; 15:57–59. [PubMed: 7022018]

25. Costarelli V, Key TJ, Appleby PN, Allen DS, Fentiman IS, Sanders TA. A prospective study of serum bile acid concentrations and colorectal cancer risk in post-menopausal women on the island of Guernsey. Br J Cancer. 2002; 86:1741–1744. [PubMed: 12087460]

26. Baker AR, McDonnell DP, Hughes M, Crisp TM, Mangelsdorf DJ, Haussler MR, Pike JW, Shine J, O'Malley BW. Cloning and expression of full-length cDNA encoding human vitamin D receptor. Proc Natl Acad Sci U S A. 1988; 85:3294–3298. [PubMed: 2835767]

27. Kamei Y, Kawada T, Fukuwatari T, Ono T, Kato S, Sugimoto E. Cloning and sequencing of the gene encoding the mouse vitamin D receptor. Gene. 1995; 152:281–282. [PubMed: 7835717]

28. Sartor RB. Microbial influences in inflammatory bowel diseases. Gastroenterology. 2008; 134:577–594. [PubMed: 18242222]

29. Cario E. Toll-like receptors in inflammatory bowel diseases: a decade later. Inflamm Bowel Dis. 2010; 16:1583–1597. [PubMed: 20803699]

30. Cario E, Podolsky DK. Differential alteration in intestinal epithelial cell expression of toll-like receptor 3 (TLR3) and TLR4 in inflammatory bowel disease. Infect Immun. 2000; 68:7010–7017. [PubMed: 11083826]

31. Akira S, Uematsu S, Takeuchi O. Pathogen recognition and innate immunity. Cell. 2006; 124:783–801. [PubMed: 16497588]

32. Yamamoto-Furusho JK, Podolsky DK. Innate immunity in inflammatory bowel disease. World J Gastroenterol. 2007; 13:5577–5580. [PubMed: 17948931]

33. Gersemann M, Becker S, Kubler I, Koslowski M, Wang G, Herrlinger KR, Griger J, Fritz P, Fellermann K, Schwab M, Wehkamp J, Stange EF. Differences in goblet cell differentiation between Crohn's disease and ulcerative colitis. Differentiation. 2009; 77:84–94. [PubMed: 19281767]

34. Zheng X, Tsuchiya K, Okamoto R, Iwasaki M, Kano Y, Sakamoto N, Nakamura T, Watanabe M. Suppression of hath1 gene expression directly regulated by hes1 via notch signaling is associated with goblet cell depletion in ulcerative colitis. Inflamm Bowel Dis. 2011; 17:2251–2260. [PubMed: 21987298]

35. Bouckenooghe T, Remacle C, Reusens B. Is taurine a functional nutrient? Curr Opin Clin Nutr Metab Care. 2006; 9:728–733. [PubMed: 17053427]

36. Son M, Ko JI, Kim WB, Kang HK, Kim BK. Taurine can ameliorate inflammatory bowel disease in rats. Adv Exp Med Biol. 1998; 442:291–298. [PubMed: 9635044]

37. Schuller-Levis G, Quinn MR, Wright C, Park E. Taurine protects against oxidant-induced lung injury: possible mechanism(s) of action. Adv Exp Med Biol. 1994; 359:31–39. [PubMed: 7534034]

38. Son MW, Ko JI, Doh HM, Kim WB, Park TS, Shim MJ, Kim BK. Protective effect of taurine on TNBS-induced inflammatory bowel disease in rats. Arch Pharm Res. 1998; 21:531–536. [PubMed: 9875490]

39. Yamada T, Grisham MB. Role of neutrophil-derived oxidants in the pathogenesis of intestinal inflammation. Klin Wochenschr. 1991; 69:988–994. [PubMed: 1665888]

40. Test ST, Lampert MB, Ossanna PJ, Thoene JG, Weiss SJ. Generation of nitrogen-chlorine oxidants by human phagocytes. J Clin Invest. 1984; 74:1341–1349. [PubMed: 6090501]

41. Delic D, Warskulat U, Borsch E, Al-Qahtani S, Al-Quraishi S, Haussinger D, Wunderlich F. Loss of ability to self-heal malaria upon taurine transporter deletion. Infect Immun. 2010; 78:1642–1649. [PubMed: 20100858]

42. Gadaleta RM, Oldenburg B, Willemsen EC, Spit M, Murzilli S, Salvatore L, Klomp LW, Siersema PD, van Erpecum KJ, van Mil SW. Activation of bile salt nuclear receptor FXR is repressed by pro-inflammatory cytokines activating NF-kappaB signaling in the intestine. Biochim Biophys Acta. 2011; 1812:851–858. [PubMed: 21540105]

43. Gadaleta RM, van Erpecum KJ, Oldenburg B, Willemsen EC, Renooij W, Murzilli S, Klomp LW, Siersema PD, Schipper ME, Danese S, Penna G, Laverny G, Adorini L, Moschetta A, van Mil SW. Farnesoid X receptor activation inhibits inflammation and preserves the intestinal barrier in inflammatory bowel disease. Gut. 2011; 60:463–472. [PubMed: 21242261]

Highlights

- *Vdr*$^{\Delta IEpC}$ mice were generated and showed changes in body mass, blood chemistry, colon structure, gene expression profile and the fecal metabolome.
- The DSS-induced colitis model was used in the *Vdr*$^{\Delta IEpC}$ mice and showed susceptibility to IBD.
- Taurine and taurine conjugated bile acids could be diagnostic biomarkers for intestinal diseases.

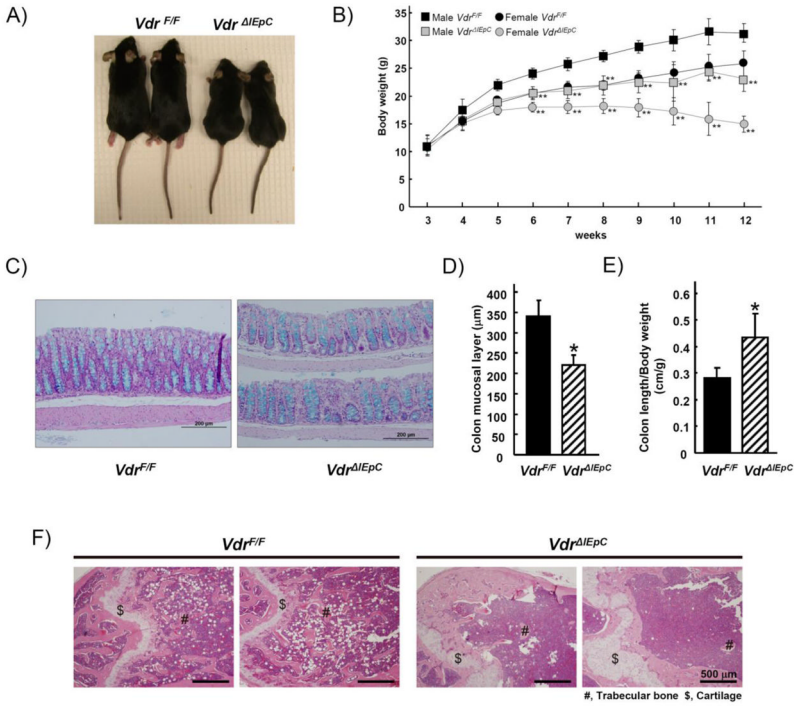

Figure 1. Phenotypes of intestine-specific *Vdr*-null mice

A) Photography shows 10 weeks old female mice having $Vdr^{F/F}$ and $Vdr^{\Delta IEpC}$ genotypes. B) Body weight changes of $Vdr^{F/F}$ (male, n= 5; female, n=6) and $Vdr^{\Delta IEpC}$ (male, n= 5; female, n=6) mice are shown in different age. C) Colons (middle) from 10-week-old male $Vdr^{F/F}$ (n= 8) and $Vdr^{\Delta IEpC}$ (n= 4) mice were stained with H&E plus Alcian blue (for goblet cells). D) Thickness of colon mucosal layer (middle) was measured from $Vdr^{F/F}$ (n= 3) and $Vdr^{\Delta IEpC}$ (n= 3) mice from the H&E stained slides using the DP Controller Program (ver. 3.1.1.267, Olympus corporation). E) Colon length from $Vdr^{F/F}$ (n= 14) and $Vdr^{\Delta IEpC}$ (n= 10) was measured. F) Distal femur were stained with H&E from 12 weeks old male $Vdr^{F/F}$ and $Vdr^{\Delta IEpC}$ mice. Duo, Duodenum; Jej, ejunum; Ile, ileum; Co, colon; Ce, cecum; Sto, stomach; Bra, brain; Ki, kidney; He, heart; Lu, lung. Data are shown as mean ± SD.*, $p < 0.00001$; **; $p < 0.0001$ compared with $Vdr^{F/F}$ mice.

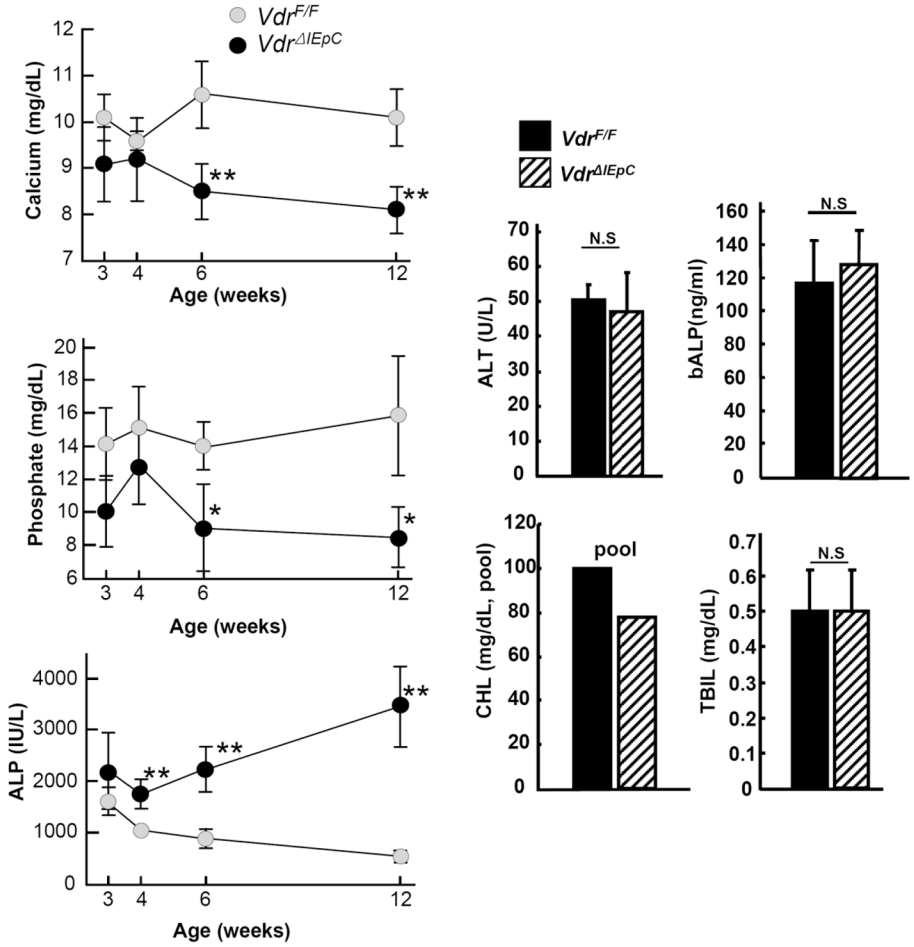

Figure 2. Serum chemistry

Calcium, phosphate and ALP levels were measured from the serum with different ages and ALT, bALP, CHL and TBIL were also measured from 11 weeks old male $Vdr^{F/F}$ (n= 6) and $Vdr^{\Delta IEpC}$ (n= 6) mice. Data are shown as mean ± SD. N.S, not significant; *, $p < 0.0001$; **, $p < 0.0002$ compared with $Vdr^{\Delta IEpC}$ mice. ALP, alkaline phosphatase; ALT, alanine aminotransferase; bALP, bone specific alkaline phoshatase CHL, cholesterol; TBIL, total bilirubin.

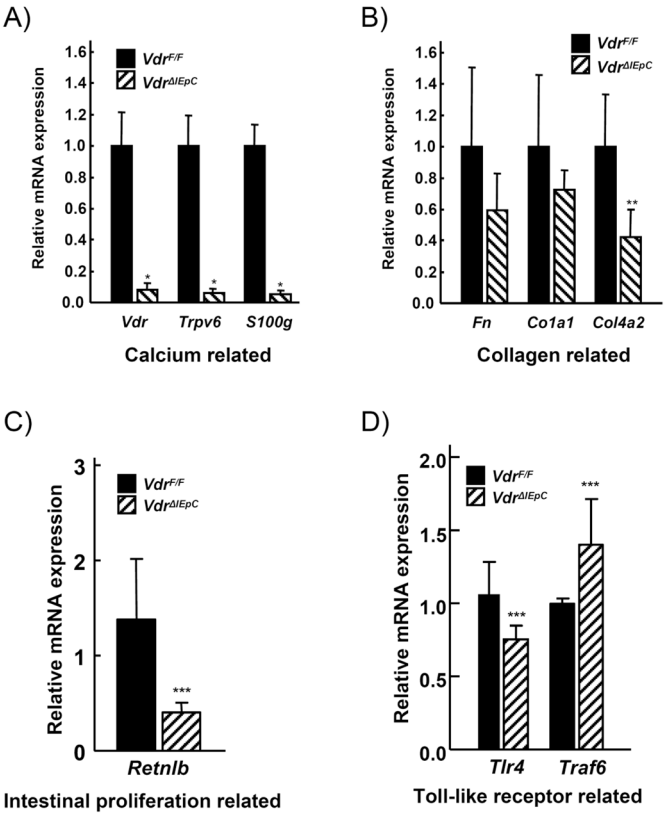

Figure 3. Gene expression changes in colon tissue from *Vdr*$^{F/F}$ and *Vdr*$^{\Delta IEpC}$ mice

qPCR was carried out for the gene analysis relating to calcium (A), collagen (B), intestinal proliferation (C) and toll-like receptor related (D)-signaling in colon tissues from *Vdr*$^{F/F}$ and *Vdr*$^{\Delta IEpC}$ mice. Data are shown as mean ± SD. *, p <0.0001; **, p < 0.03; ***, p < 0.2 compared with *Vdr*$^{F/F}$ mice.

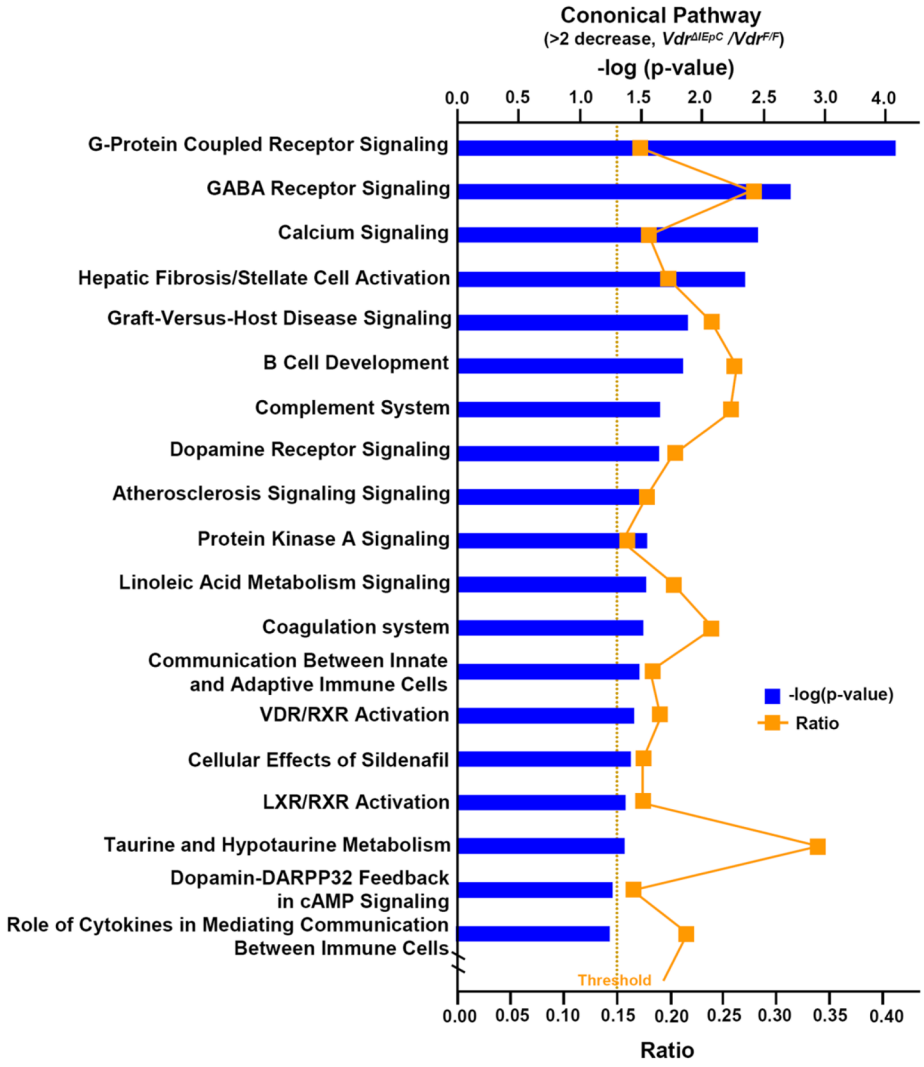

Figure 4. Cononical pathway from microarray analysis

The ratio and –log (p-value) are shown from over 2-fold gene decrease in $Vdr^{\Delta IEpC}$.

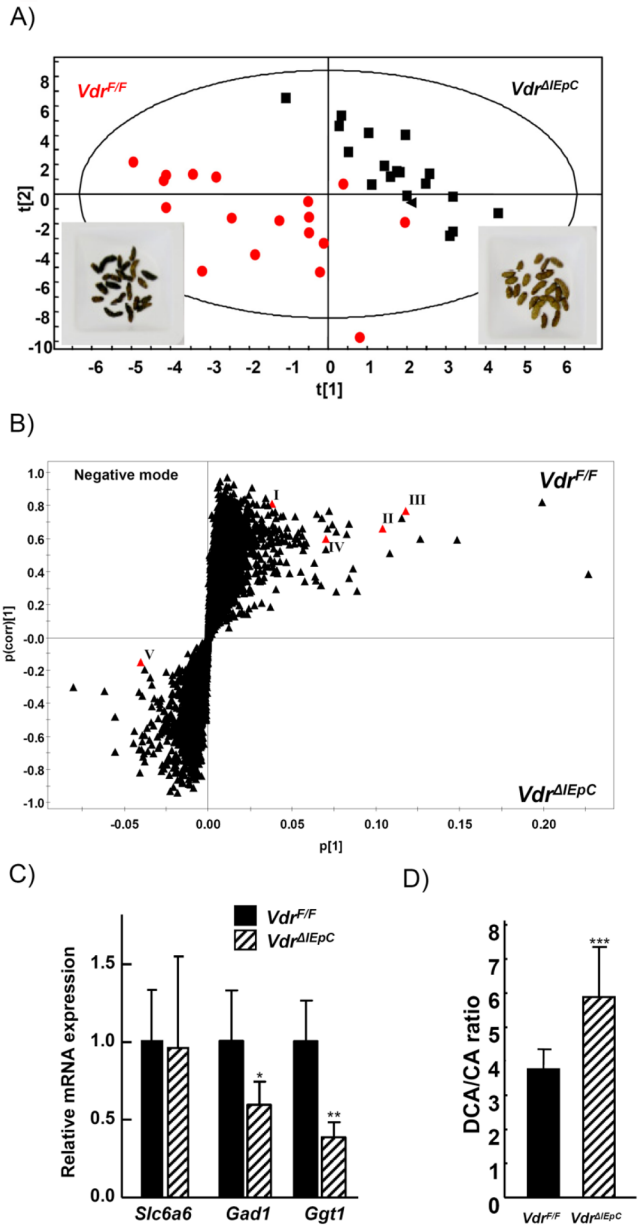

Figure 5. Metabolomics from the mouse feces

A) Partial least squares discriminant analysis (PLS-DA) scores plot from 10 week old male *Vdr*$^{F/F}$ (n= 6) and *Vdr*$^{\Delta IEpC}$ (n= 6) mouse feces analyzed by UPLC-ESI-QTOFMS ESI- mode. B) OPLS-DA loadings S-plot from the same samples in (A). C) Taurine transporter, *Slc6a6* mRNA and taurine metabolism related genes, *Gad1* and *Ggt1*, were measured by qPCR. D) DCA/CA ratio. DCA, deoxycholic acid; CA, cholic acid. Data are shown as mean ± SD. *, p=0.29; **, p <0.07; ***, p < 0.01 compared with *Vdr*$^{F/F}$ mice. I, taurine; II, taurocholic acid; III, taurodeoxycholic acid; IV, cholic acid; V, deoxycholic acid

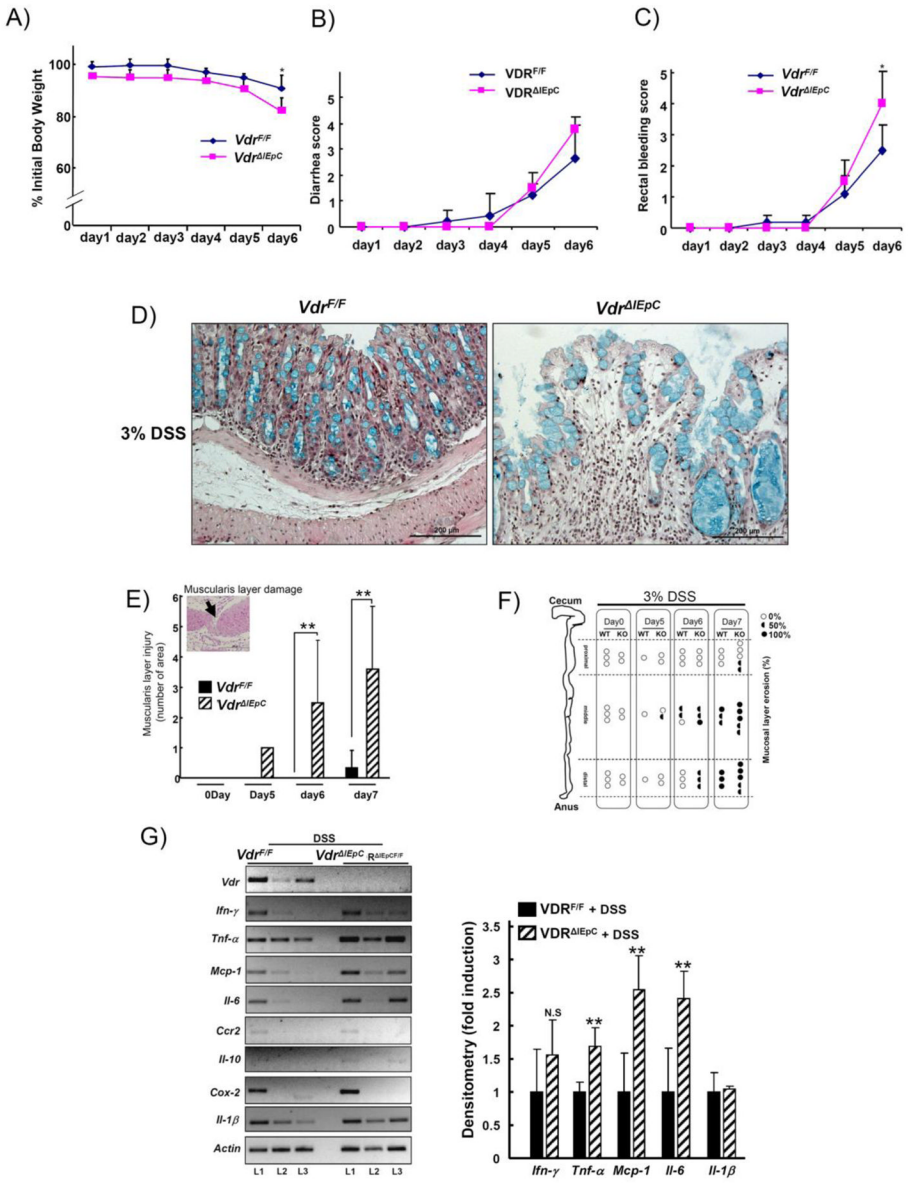

Figure 6. Acute induction of colitis by treatment with DSS

Ten week-old male *Vdr*$^{F/F}$ (n= 8) and *Vdr*$^{\Delta IEpC}$ (n= 7) mice were treated with 3% DSS for 6 or 7 day. A) Percent initial body weight, B) Diarrhea score and C) Rectal bleeding score were measured. D) Colon (distal) histology was assessed from *Vdr*$^{F/F}$ (n= 3) and *Vdr*$^{\Delta IEpC}$ (n= 3) mice by H&E plus Alcian blue staining. E) Muscularis layer damage was evaluated by counting the damaged areas. F) Erosive mucosal layers after 3% DSS treatment were assessed from the each mouse. Open circle, closed semicircle and closed circle represent as 0%, 50% and 100% erosive, respectively. WT, *Vdr*$^{F/F}$; KO, *Vdr*$^{\Delta IEpC}$. G) Cytokine and inflammatory related gene expressions were analyzed from *Vdr*$^{F/F}$ (n= 3) and *Vdr*$^{\Delta IEpC}$ (n= 3) mice using the RT-PCR method. Data are shown as mean ± SD. *, $p < 0.001$, **, $p < 0.05$ compared with *Vdr*$^{F/F}$ mice.

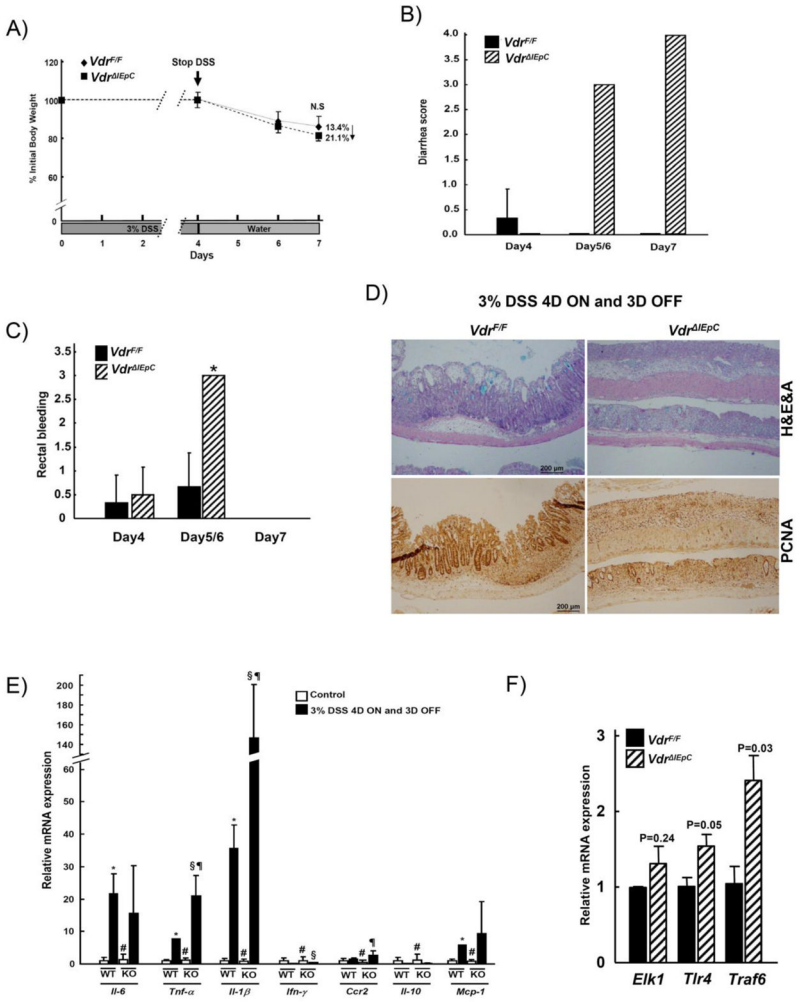

Figure 7. Recovery of colitis from the DSS treatment

Ten week-old male $Vdr^{F/F}$ (n= 7) and $Vdr^{\Delta IEpC}$ (n= 6) mice were treated with 3% DSS for 4 days and replaced to water for another 3 days. A) Percent initial body weight, B) Diarrhea score and C) Rectal bleeding score were measured. D) Colon histology was assessed by H&E plus Alcian blue staining and immunohistochemistry. E) Cytokine and inflammatory related gene expressions were analyzed by qPCR. F) Toll-like receptor related mRNAs were measured. L, litermate. Data are shown as mean ± SD. #, N.S; *, $p < 0.001$ (Control $VDR^{F/F}$ *vs* DSS $VDR^{F/F}$); §, $p < 0.02$ (Control $Vdr^{F/F}$ *vs* DSS $Vdr^{\Delta IEpC}$); ¶, $p < 0.01$ (DSS $Vdr^{\Delta IEpC}$ *vs* DSS $Vdr^{\Delta IEpC}$).